G. M. HAMILTON[1]
Research Laboratory,
Associated Electrical Industries,
Aldermaston, Berkshire, England

L. E. GOODMAN
Professor and Head,
Department of Civil Engineering
and Hydraulics,
University of Minnesota,
Minneapolis, Minn. Mem. ASME

The Stress Field Created by a Circular Sliding Contact

Equations are obtained for the complete stress field due to a circular contact region carrying a "hemispherical" Hertzian normal pressure and a proportional distributed shearing traction. The equations are illustrated by graphs of a constant-yield parameter and graphs of maximum tensile stress.

MEASUREMENTS of the frictional properties of material surfaces are commonly made by rubbing a lightly loaded spherical slider over a flat of the material being tested. The quasi-static stress field so generated is the sum of two determined by the field equations of the linear theory of elasticity and by the boundary conditions on the plane $z = 0$ of the half space $z > 0$:

$$p_{yz} = p_{zz} = 0; \quad p_{xz} = -(3fP/2\pi a^3)(a^2 - r^2)^{1/2}, \qquad r < a \quad (1)$$

$$p_{yz} = p_{xz} = 0; \quad p_{zz} = -(3P/2\pi a^3)(a^2 - r^2)^{1/2} \qquad r < a. \quad (2)$$

All traction on $z = 0$ is to vanish for $r > a$ and all stresses decay to zero at least as rapidly as $(x^2 + y^2 + z^2)^{-1}$ at points remote from the origin. In (1, 2), $r = (x^2 + y^2)^{1/2}$, a is the radius of the loaded region, P is the total normal load, and fP is the x-directed total tangential force, Fig. 1. These conditions have been discussed by Mindlin [1],[2] Cattaneo [5], and Sonntag [6].

This same stress field is also generated by crossed-cylinder lubricant research apparatus. Moreover, it represents quite closely the state of affairs near each of the several load-bearing asperities between a large pair of sliding surfaces. The stresses generated, in many instances, govern the onset of surface failure.

Method of Analysis

In principle, all that is necessary for a formal determination of the stress field is to write down the expressions for the state of stress due to the application of a point force (half-space solutions of Boussinesq and Cerutti) and to integrate over the plane $z = 0$ with the appropriate weighting functions given by (1, 2). Unfortunately, this direct approach leads to a series of intractable integrals. The analysis may, however, be carried out by an extension to the shear-loaded half space of a method introduced by A. E. Green [2] for the stress analysis of the normally loaded half space. This extension has the advantage of being equally applicable to the mixed boundary-value problem in which a combination of displacements and stress components is specified on $z = 0$.

To effect the extension, we write the Cartesian displacement components u, v, w in terms of a harmonic stress function $T(x, y, z)$:

$$2\mu u = 2\nu(\partial^2 T/\partial x^2) + 2(\partial^2 T/\partial z^2) - z(\partial^3 T/\partial x^2 \partial z) \quad (3a)$$

$$2\mu v = 2\nu(\partial^2 T/\partial x \partial y) - z(\partial^3 T/\partial x \partial y \partial z) \quad (3b)$$

$$2\mu w = (1 - 2\nu)(\partial^2 T/\partial x \partial z) - z(\partial^3 T/\partial x \partial z^2) \quad (3c)$$

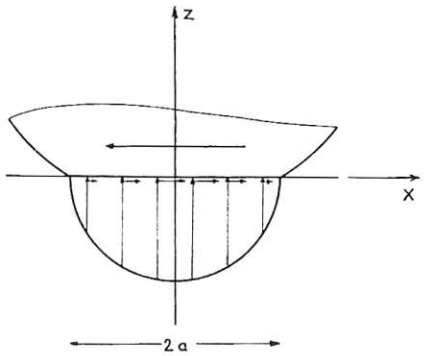

Fig. 1 Schematic view of contact. Equations apply to upper body for which normal force is in positive z-direction and tangential force in positive x-direction

where μ is the shear modulus and ν is Poisson's ratio. The field equations of the linear theory of elasticity and the first two boundary conditions (1) are then automatically satisfied. By taking T as the imaginary part of the complex harmonic function

$$\int_0^a t(\xi) \left\{ \frac{1}{2}\left(z_1^2 - \frac{1}{2} r^2\right) \ln (z_1 + R_1) - \frac{3}{4} R_1 z_1 + \frac{1}{4} r^2 \right\} d\xi \quad (4)$$

where $z_1 = z + i\xi$ and $R_1 = (z_1^2 + r^2)^{1/2}$; the plane $z = 0$ is automatically cleared of traction for $r > a$.

It remains to choose $t(\xi)$ so as to satisfy the last of boundary conditions (1). On $z = 0$ for $r < a$, equations (3, 4) imply that

$$p_{xz} = \int_r^a t(\xi)(\xi^2 - r^2)^{-1/2} d\xi \quad (5)$$

so that

$$t(\xi) = \frac{-2}{\pi} \frac{d}{d\xi} \int_\xi^a r p_{xz} (r^2 - \xi^2)^{-1/2} dr. \quad (6)$$

For p_{xz} given by the third of boundary conditions (1), $t(\xi) = -(3fP/2\pi a^3)\xi$.

The determination of the stress field then follows from (3, 4) by elementary quadratures. We find that, writing $z_2 = z + ia$ and $R_2 = (z_2^2 + r^2)^{1/2}$, the stress components are conveniently expressed in terms of the imaginary parts of three complex functions:

$$F = \tfrac{1}{2}(z - ia)R_2 + \tfrac{1}{2}r^2 \ln (R_2 + z_2) \quad (7a)$$

$$G = -\tfrac{1}{3}R_2^3 + \tfrac{1}{2}zz_2R_2 - \tfrac{1}{3}ia^3 + \tfrac{1}{2}zr^2 \ln (R_2 + z_2) \quad (7b)$$

$$H = \tfrac{4}{3}ia^3z - \tfrac{1}{6}zR_2^3 + \tfrac{1}{2}iaR_2^3 - \tfrac{1}{4}z_2R_2r^2 - \frac{r^4}{4} \ln (R_2 + z_2). \quad (7c)$$

[1] Now at J. J. Thomson Physical Laboratory, The University, Whiteknights Park, Reading, England.

[2] Numbers in brackets designate References at end of paper.

Presented at the Fifth U. S. National Congress of Applied Mechanics, University of Minnesota, Minneapolis, Minn., June 14–17, 1966.

Discussion of this paper should be addressed to the Editorial Department, ASME, United Engineering Center, 345 East 47th Street, New York, N. Y. 10017, and will be accepted until July 10, 1966. Discussion received after the closing date will be returned. Manuscript received by ASME Applied Mechanics Division, September 30, 1964; final draft, May 26, 1965.

The Cartesian components of the stress field generated by (1) are the imaginary parts of

$$p_{xx} = \frac{3fP}{2\pi a^3}\frac{x}{r^4}\left[\left(4\frac{x^2}{r^2}-3\right)\left(H\nu-\frac{1}{2}z\frac{\partial H}{\partial z}\right)+y\frac{\partial H}{\partial y}+(1-\nu)x\frac{\partial H}{\partial x}+\frac{1}{2}xz\frac{\partial^2 H}{\partial x\partial z}-2\nu r^2F\right] \quad (8a)$$

$$p_{yy} = \frac{3fP}{2\pi a^3}\frac{x}{r^4}\left[\left(4\frac{y^2}{r^2}-1\right)\left(H\nu-\frac{1}{2}z\frac{\partial H}{\partial z}\right)-\nu y\frac{\partial H}{\partial y}+\frac{1}{2}yz\frac{\partial^2 H}{\partial y\partial z}-2\nu r^2F\right] \quad (8b)$$

$$p_{zz} = \frac{3fP}{2\pi a^3}\frac{xz}{r^2}\frac{\partial F}{\partial z};\quad p_{yz} = \frac{3fP}{2\pi a^3}\frac{xyz}{2r^4}\frac{\partial^2 H}{\partial z^2} \quad (8c, d)$$

$$p_{xz} = \frac{3fP}{2\pi a^3}\frac{1}{r^2}\left[2G+\frac{1}{2}\frac{\partial H}{\partial z}+z\frac{\partial}{\partial x}(xF)-2\frac{zx^2}{r^2}F\right] \quad (8e)$$

$$p_{xy} = \frac{3fP}{2\pi a^3}\frac{y}{r^4}\left[\left(4\frac{x^2}{r^2}-1\right)\left(H\nu-\frac{1}{2}z\frac{\partial H}{\partial z}\right)+\frac{1}{2}y\frac{\partial H}{\partial y}+\frac{1}{2}x(1-2\nu)\frac{\partial H}{\partial x}+\frac{1}{2}zx\frac{\partial^2 H}{\partial x\partial z}\right]. \quad (8f)$$

On the z-axis the only nonvanishing stress component is

$$p_{zz} = (3fP/2\pi a^3)[\tfrac{3}{2}z\arctan(a/z) - a - \tfrac{1}{2}az^2(z^2+a^2)^{-1}]. \quad (9)$$

On the surface inside the contact zone, i.e., $z = 0$, $r < a$, the stress components other than those given by (1) are

$$p_{yy} = [3\nu/(4+\nu)]p_{xx} = (x/y)[3\nu/(2-\nu)]p_{xy} = -(3fP/2\pi a^3)\tfrac{3}{8}x\nu \quad (10)$$

while on the surface outside the contact zone

$$p_{xx} = -(3fP/2\pi a^3)(xr^{-4})[2(r^2+\nu y^2)F_0 + \nu(3-4x^2r^{-2})H_0] \quad (11a)$$

$$p_{yy} = -(3fP/2\pi a^3)(\nu x r^{-4})[2x^2F_0 + (1-4y^2r^{-2})H_0] \quad (11b)$$

$$p_{xy} = -(3fP/2\pi a^3)(yr^{-4})[(r^2-2\nu x^2)F_0 + \nu(1-4x^2r^{-2})H_0] \quad (11c)$$

where

$$F_0 = -\tfrac{1}{2}a(r^2-a^2)^{1/2} + \tfrac{1}{2}r^2\arctan[a(r^2-a^2)^{-1/2}] \quad (11d)$$

$$H_0 = \tfrac{1}{2}a(r^2-a^2)^{3/2} - \tfrac{1}{4}r^4\arctan[a(r^2-a^2)^{-1/2}] - \tfrac{1}{4}ar^2(r^2-a^2)^{1/2}. \quad (11e)$$

Determination of the stress field generated by the boundary conditions (2) requires no extension of Green's method; one has only to derive displacements from a harmonic stress function $M(x, y, z)$ according to the rules

$$2\mu u = -(1-2\nu)(\partial^2 M/\partial x\partial z) - z(\partial^3 M/\partial x\partial z^2) \quad (12a)$$

$$2\mu v = -(1-2\nu)(\partial^2 M/\partial y\partial z) - z(\partial^3 M/\partial y\partial z^2) \quad (12b)$$

$$2\mu w = 2(1-\nu)(\partial^2 M/\partial z^2) - z(\partial^3 M/\partial z^3) \quad (12c)$$

and proceed as before. As the case (2) has been treated by Huber [3] (though in a less usable form), we merely state the relevant results. It is convenient to introduce the imaginary part of the complex function

$$K = z\ln\{z+ia+[r^2+(z+ia)^2]^{1/2}\} - [r^2+(z+ia)^2]^{1/2}. \quad (13)$$

Then boundary conditions (2) generate the stress field

$$p_{xx} = (3P/2\pi a^3)[2\nu K + (1-2\nu)r^{-4}(y^2G - x^2G + xr^2\partial G/\partial x) + zr^{-4}(y^2F - x^2F + xr^2\partial F/\partial x)] \quad (14a)$$

$$p_{yy} = (3P/2\pi a^3)[2\nu K + (1-2\nu)r^{-4}(x^2G - y^2G + yr^2\partial G/\partial y) + zr^{-4}(x^2F - y^2F + yr^2\partial F/\partial y)] \quad (14b)$$

$$p_{zz} = -(3P/2\pi a^3)(-K + z\partial K/\partial z)$$

$$p_{yz} = -(3P/2\pi a^3)z\partial K/\partial y;\quad p_{xz} = -(3P/2\pi a^3)z\partial K/\partial x \quad (14c)$$

$$p_{xy} = (3P/2\pi a^3)(xr^{-4})[(1-2\nu)(-2yG + r^2\partial G/\partial y) + z(-2yF + r^2\partial F/\partial y)]. \quad (14d)$$

On the z-axis

$$p_{xx} = p_{yy} = (3P/2\pi a^3)\{(1+\nu)[z\arctan(a/z) - a] + \tfrac{1}{2}a^3/(a^2+z^2)\} \quad (15a)$$

$$p_{zz} = -(3P/2\pi a^3)[a^3/(a^2+z^2)]. \quad (15b)$$

On the surface inside the zone of contact

$$p_{xx} = (3P/2\pi a^3)[2\nu K_0 + (1-2\nu)(G_0r^{-2} - 2x^2r^{-4}G_0 + x^2r^{-2}K_0)] \quad (16a)$$

$$p_{yy} = (3P/2\pi a^3)[2\nu K_0 + (1-2\nu)(G_0r^{-2} - 2y^2r^{-4}G_0 + y^2r^{-2}K_0)] \quad (16b)$$

$$p_{xy} = (3P/2\pi a^3)(1-2\nu)(xyr^{-2}K_0 - 2xyr^{-4}G_0) \quad (16c)$$

while outside the zone of contact

$$p_{xx} = (3P/2\pi a^3)(\tfrac{1}{3}a^3(1-2\nu)(2x^2r^{-4} - r^{-2})] \quad (17a)$$

$$p_{yy} = (3P/2\pi a^3)[\tfrac{1}{3}a^3(1-2\nu)(2y^2r^{-4} - r^{-2})] \quad (17b)$$

$$p_{xy} = (3P/2\pi a^3)[\tfrac{2}{3}a^3(1-2\nu)xyr^{-4}] \quad (17c)$$

where

$$G_0 = \tfrac{1}{3}(a^2-r^2)^{3/2} - \tfrac{1}{3}a^3;\quad K_0 = -(a^2-r^2)^{1/2}. \quad (17d)$$

Discussion

The stress field created by a circular sliding contact is mainly of interest in connection with questions of mechanical failure. The quantities of greatest interest, then, are the position of any region of failure predicted by a yield criterion and the appearance of large tensile stresses, particularly in the surface. In the diagrams which follow, the unit of distance is the radius of the circle of contact, given by

$$a = \{\tfrac{3}{8}P(R_1^{-1}+R_2^{-1})^{-1}[(1-\nu_1)/\mu_1 + (1-\nu_2)/\mu_2]\}^{1/3} \quad (18)$$

and the unit of stress is the maximum pressure at the center of the contact:

$$p_0 = 3P/2\pi a^2. \quad (19)$$

The suffixes 1, 2 refer to individual properties of the two bodies in contact. Poisson's ratio has been taken as 0.3 in the examples.

Plastic Yielding. This can be predicted by the von Mises yield criterion, the square root of the second invariant of the stress deviator tensor. In Cartesian form, this may be written

$$J_2 = p_{xy}^2 + p_{xz}^2 + p_{xy}^2 + \tfrac{1}{6}[(p_{yy}-p_{zz})^2 + (p_{zz}-p_{xx})^2 + (p_{xx}-p_{yy})^2] \quad (20)$$

with yielding occurring when $(J_2)^{1/2}$ reaches the material yield point in simple shear. Equation (20) was evaluated on the plane $y = 0$ for a number of coefficients of friction and the results are shown in Figs. 2, 3, and 4. For $f = 0$, the diagram shows the well-known result that the region of maximum yield parameter occurs on the centerline a distance $0.5a$ below the surface. Figs. 3 and 4 show the effect of increasing the friction to 0.25 and 0.50.

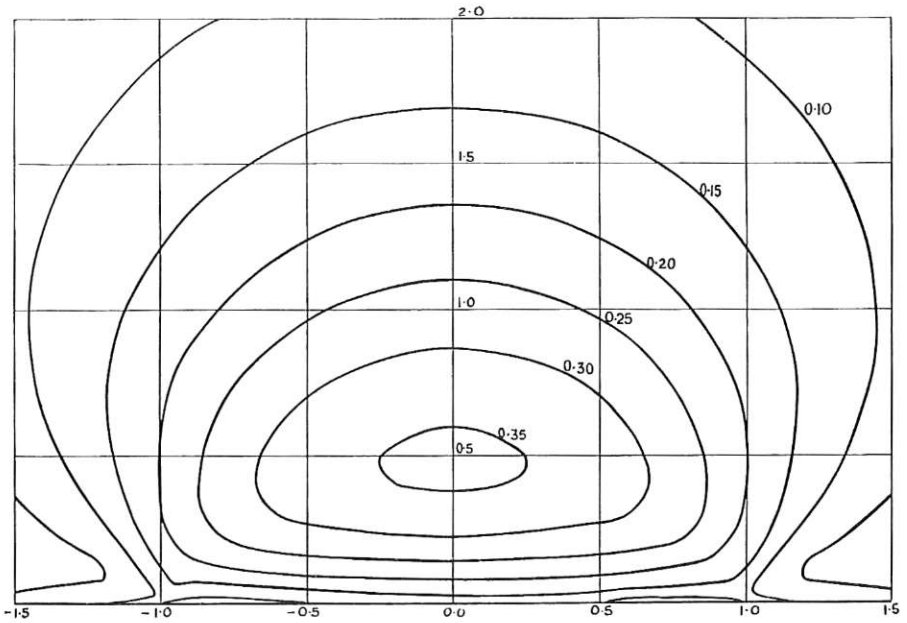

Fig. 2 Lines of constant $J_2^{1/2}/p_0$ on plane $y = 0$ beneath normally loaded circular contact

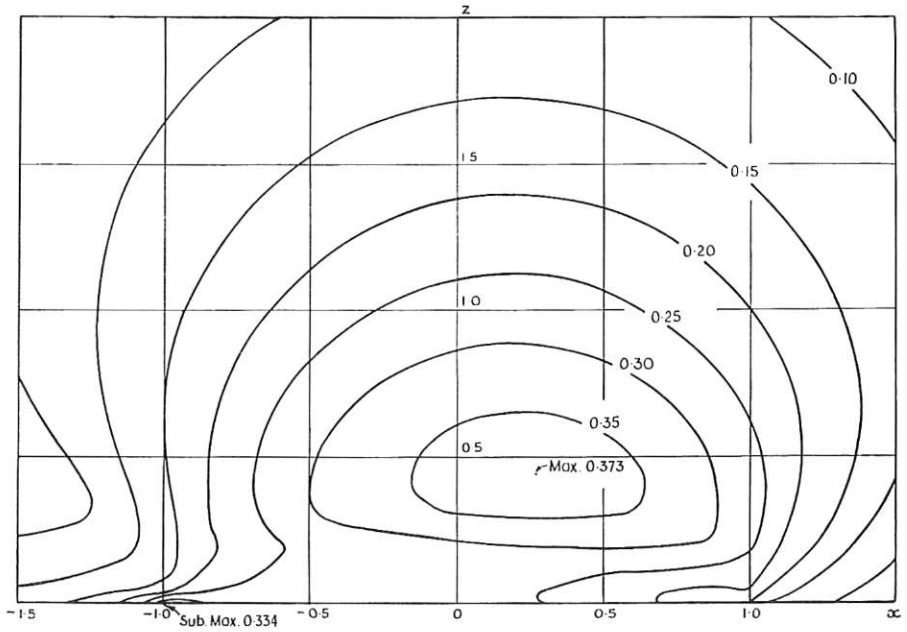

Fig. 3 Lines of constant $J_2^{1/2}/p_0$ on plane $y = 0$ beneath circular contact, $f = 0.25$

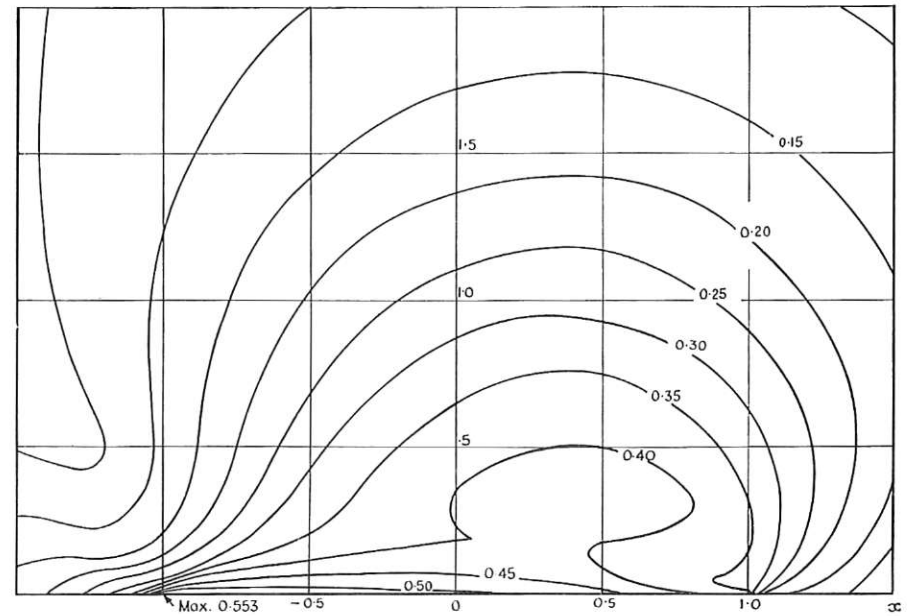

Fig. 4 Lines of constant $J_2^{1/2}/p_0$ on plane $y = 0$ beneath circular contact, $f = 0.50$

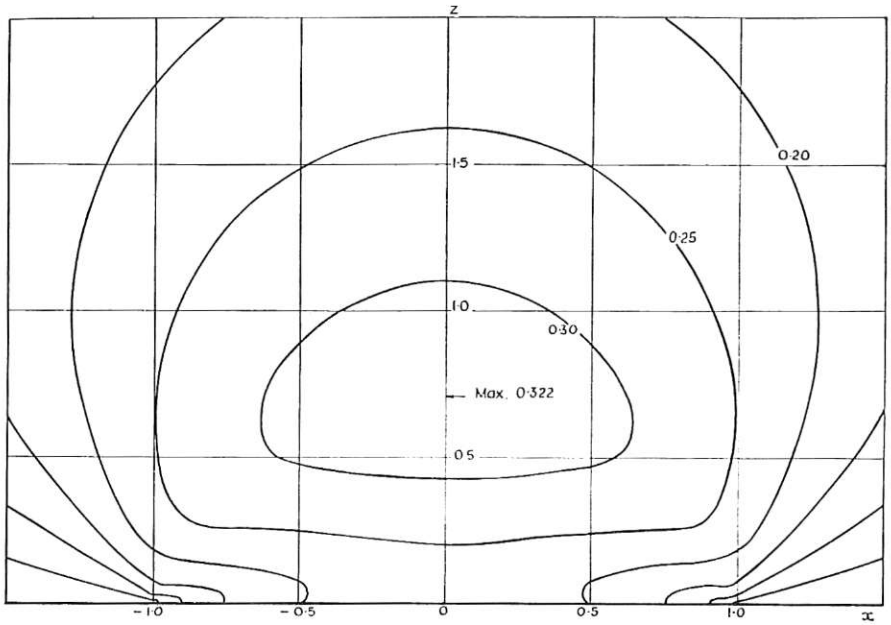

Fig. 5 Lines of constant $J_2^{1/2}/p_0$ beneath contact between normally loaded cylinders

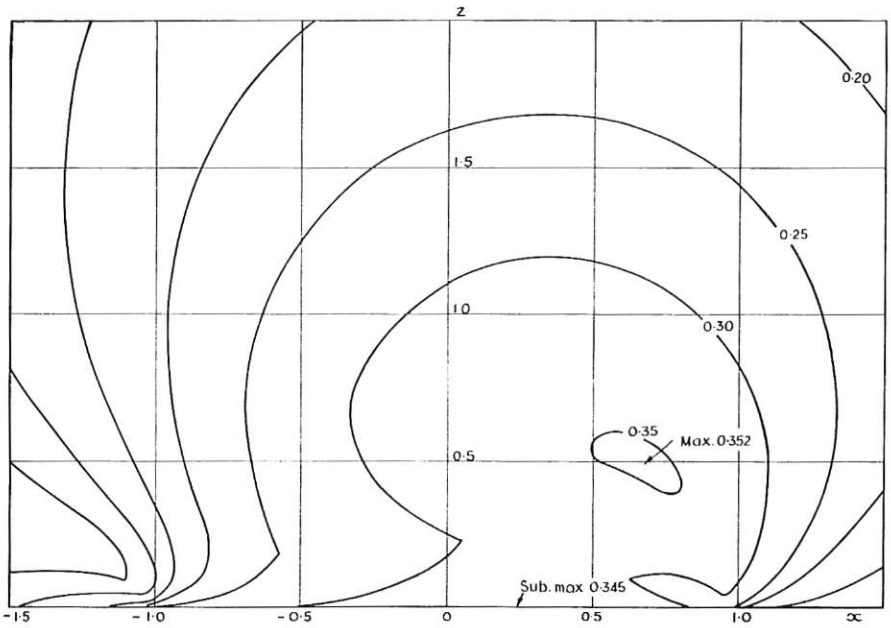

Fig. 6 Lines of constant $J_2^{1/2}/p_0$ beneath contact between cylinders, $f = 0.25$

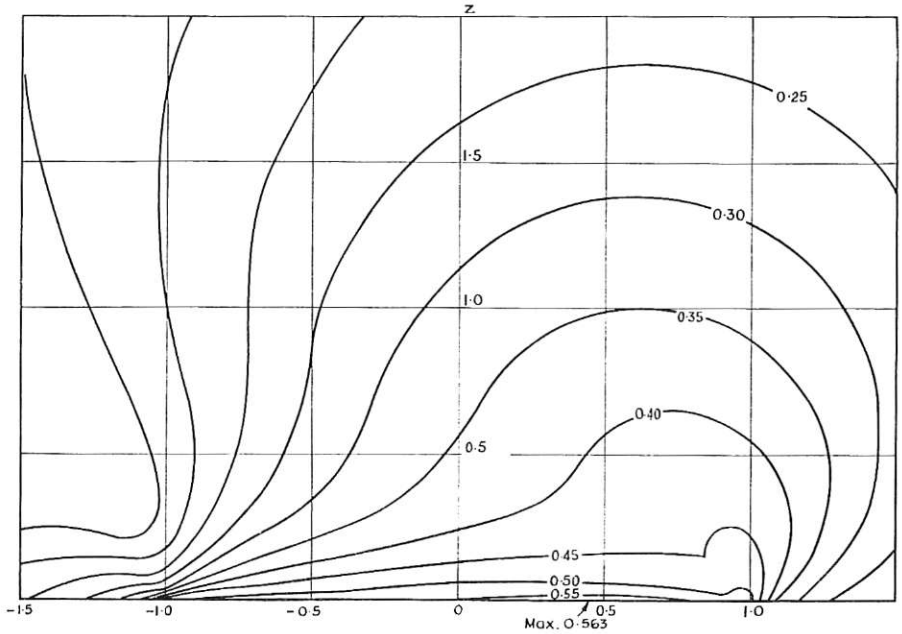

Fig. 7 Lines of constant $J_2^{1/2}/p_0$ beneath contact between cylinders, $f = 0.50$

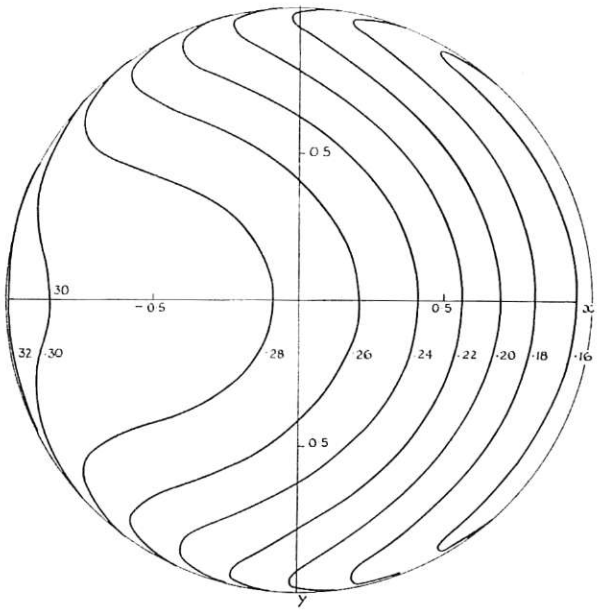

Fig. 8 Lines of constant $J_2^{1/2}/p_0$ in surface of circular contact, $f = 0.25$

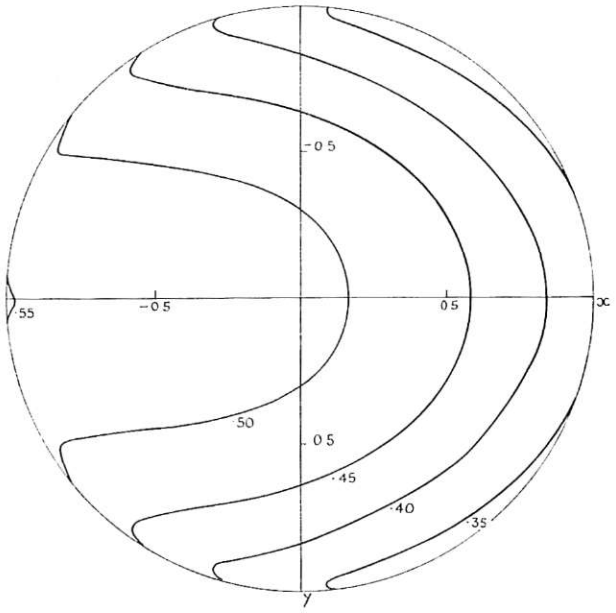

Fig. 9 Lines of constant $J_2^{1/2}/p_0$ in surface of circular contact, $f = 0.50$

The region of maximum yield parameter moves toward the surface and becomes more intense while simultaneously a second region of high yield stress develops in the surface at $x = -1.0a$. The point of maximum yield stress changes from below the surface to a position on the surface at a coefficient of friction about 0.27.

It has been customary to assume that conditions on the center plane of a circular contact are similar to the equivalent case of a cylindrical contact. For comparison, Figs. 5, 6, and 7 show the same three examples, $f = 0$, 0.25 and 0.50, worked out for cylinders in line contact using the equations given by Poritsky [4] and assuming a state of plane strain; i.e., $p_{yy} = \nu p_{xx} + \nu p_{zz}$. The relation between contact width and maximum pressure is now $p_0 = 2P/\pi a$.

The region of maximum yield parameter moves toward the surface in both cases as the friction is increased, but rather less rapidly in the case of a circular contact. The second region of shear stress develops on the opposite side of the centerline and at the edge of the contact, a fact that may affect the stability of a system when failure is imminent, especially for failure mechanisms where small changes of temperature are important.

For this reason, two further views of the circular contact are shown as Figs. 8 and 9. These are plan views of the contact and show the shape of the region of maximum yield parameter which develops in the surface. The case $f = 0$ is not shown since it merely consists of a series of concentric circles the diameters of which may be obtained from Fig. 2.

Tensile Stresses. With brittle materials the appearance of tensile stresses is more important than the value of the yield parameter. Even when the coefficient of friction is zero, one of the principal stresses in the surface is tensile near the edge of the contact. This stress acts in a radial direction and accounts for the well-known ring crack. Fig. 10 shows a graph of this stress along the centerline $y = z = 0$ where it coincides with p_{xx}. As the coefficient of friction increases, p_{xx} ceases to be a principal stress but it is still the largest tensile stress acting in the plane of the surface. The stress becomes unsymmetrical, compressive at the rear of the contact and greatly intensified at the front. The completely closed ring of tensile stress around the circumference breaks at $f = 0.079$; by $f = 0.50$, the tensile stresses at the front edge of the contact have risen so high as to be equal to the compressive stress at the center.

Off the centerline, the maximum tensile stress acting in the plane of the surface is given by

$$\bar{p} = \tfrac{1}{2}(p_{xx} + p_{yy}) + \tfrac{1}{2}[(p_{xx} - p_{yy})^2 + 4p_{xy}^2]^{1/2} \qquad (21)$$

and lines of constant $\bar{p}$ are shown in Figs. 11 and 12 for $f = 0.25$ and 0.50. The direction this stress makes with the x-axis is

$$\theta = \tfrac{1}{2} \arctan [2p_{xy}/(p_{xx} - p_{yy})] \qquad (22)$$

This direction is shown by arrows at a few selected points, the base of the arrow being the point of reference. That this system of tensile stresses is very shallow can be seen from Fig. 13 which shows the the maximum principal stress on a section through the centerline, i.e., in the plane $y = 0$, for the same three coefficients of friction. Also shown on Fig. 13 are the 90-deg isoclinics originating from the point of maximum tensile stress. These are likely to control the initial direction of propagation of a crack.

Conclusion

The equations have been derived for the stresses beneath a

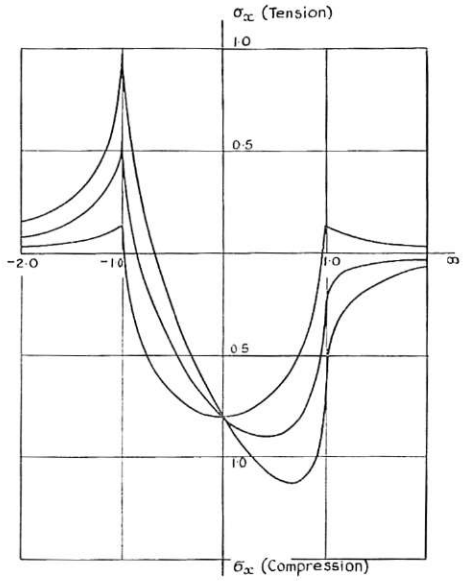

Fig. 10 Stress p_{xx} along x-axis of circular contact for $f = 0.25$, 0.50

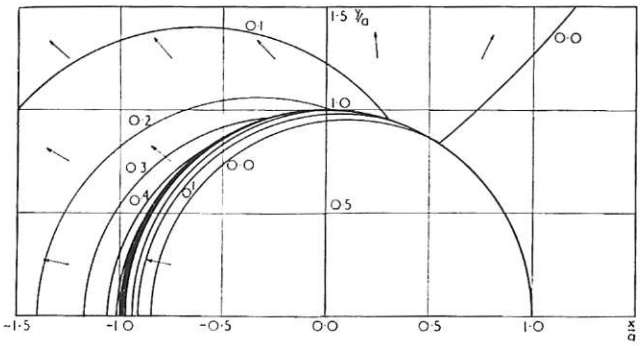

Fig. 11 Lines of constant tensile stress acting in plane of contact, f = 0.25

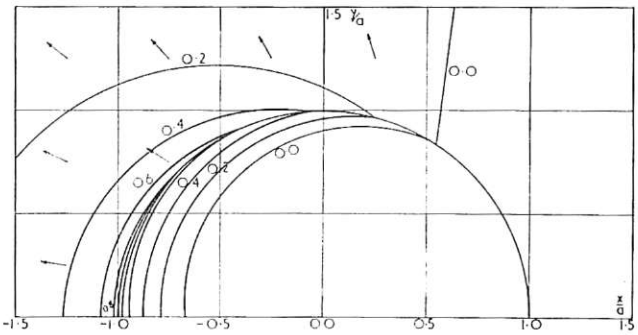

Fig. 12 Lines of constant tensile stress acting in plane of contact, f = 0.50

circular region of contact subject to a normal and a tangential force distributed "hemispherically" over the surface. They have been illustrated by graphs of yield parameter and tensile-stress distribution, and it has been concluded that the most likely region of failure is the front edge of the circle of contact.

Acknowledgments

Thanks are due to Dr. W. Hirst for many helpful suggestions and to Dr. T. E. Allibone, C.B.E., F.R.S., Director of the A.E.I. Research Laboratory for permission to publish this paper. One of the authors (L.E.G.) acknowledges with grateful thanks the support of the National Science Foundation during the period of this work.

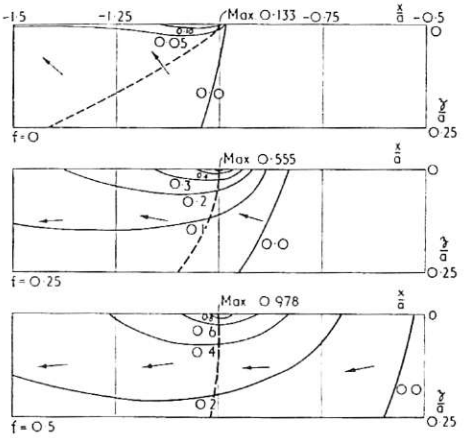

Fig. 13 One of two principal stresses on plane y = 0 in region where it is in tension, f = 0, 0.25, 0.50

References

1 R. D. Mindlin," Compliance of Elastic Bodies in Contact," JOURNAL OF APPLIED MECHANICS, vol. 16, TRANS. ASME, vol. 71, 1949, p. 259.

2 A. E. Green, "On Boussinesq's Problem and Penny-Shaped Cracks," *Proceedings of the Cambridge Philosophical Society*, vol. 45, 1949, pp. 251–257.

3 M. T. Huber, "Zur Theorie der Beruhrung fester elastischer Korper," *Annalen der Physik*, Leipzig, Germany, vol. 14, 1904, pp. 153–163. A misprint occurs in equation (10) of Huber's paper. The fourth term should read $(1 - \mu)\, u/(a^2 + u)$.

4 H. Poritsky, "Stresses and Deflections of Cylindrical Bodies With Application to Contact of Gears and of Locomotive Wheels," JOURNAL OF APPLIED MECHANICS, vol. 17, TRANS. ASME, vol. 72, 1950, pp. 191–201.

5 C. Cattaneo, "Sul contatto di due corpi elastici: distribuzione locale degli storzi," *Rendiconti dell'Accademia nazionale dei Lincei*, vol. 27, Series 6, 1938, pp. 342–348, 434–436, 474–478.

6 G. Sonntag, *Zeitschrift für angewandte Mathematik und Mechanik*, vol. 29, 1949, pp. 52–54.